Biochemical and Biophysical Research Communications 464 (2015) 168–175

Contents lists available at ScienceDirect

Biochemical and Biophysical Research Communications

journal homepage: www.elsevier.com/locate/ybbrc

RGS19 converts iron deprivation stress into a growth-inhibitory signal

Junmo Hwang [a], Hyeng-Soo Kim [a], Beom Sik Kang [a], Do-Hyung Kim [b], Zae Young Ryoo [a], Sang-Un Choi [c], Sanggyu Lee [a, *]

[a] School of Life Sciences, BK21 Plus KNU Creative BioResearch Group, Kyungpook National University, Daegu 702-701, Republic of Korea
[b] School of Physics and Energy Science, Kyungpook National University, Daegu 702-701, Republic of Korea
[c] Korea Research Institute of Chemical Technology, Daejeon 305-600, Republic of Korea

ARTICLE INFO

Article history:
Received 6 June 2015
Accepted 16 June 2015
Available online 23 June 2015

Keywords:
Regulator of G-protein signaling
N-myc downstream-regulated gene 1 protein
Cysteine string motif
Iron-binding protein

ABSTRACT

Iron chelation is a promising therapeutic strategy for cancer that works, in part, by inducing overexpression of N-myc downstream-regulated gene 1 protein (NDRG1), a known growth inhibitor and metastasis suppressor. However, details of the signaling cascades that convert physical stress into a biological response remain elusive. We investigated the role of RGS19, a regulator of G-protein signaling, in iron chelator-induced NDRG1 overexpression in HeLa cells. Knockdown of RGS19 diminished the expression of genes involved in desferrioxamine (DFO)-induced growth inhibition. Conversely, overexpression of RGS19 enhanced the expression of these genes. Moreover, overexpression of RGS19 reduced cell viability. Overexpression of G-protein alpha subunit i3 (Gαi3) repressed the induction of NDRG1 expression. Selective inhibition of downstream targets of Gαi3 abrogated DFO-induced overexpression of NDRG1. DFO protected RGS19 from proteolysis induced by GAIP interacting protein N terminus (GIPN); moreover, an iron-deficient RGS19 mutant was stable in the presence of GIPN and retained GTPase-activating protein activity. RGS19 was co-purified with iron and showed unique UV-absorption characteristics frequently observed in iron-binding proteins. This study demonstrates that RGS19 senses cellular iron availability and is stabilized under iron-depleted conditions, resulting in the induction of a growth-inhibitory signal.

1. Introduction

Iron is fundamental to DNA synthesis, cellular respiration, energy metabolism, and protein activation. Cancer cells have a high iron uptake to maintain their rapid proliferation [1]. Consequently, iron chelation is widely considered a plausible approach for effective treatment of several cancers [2].

N-myc downstream-regulated gene 1 protein (NDRG1) is a well-known prognostic marker; its low expression predicts a poor outcome in patients with cancer [3]. In addition, it increases the expression of p21, a cyclin-dependent kinase inhibitor [4]. Iron chelators significantly increase the expression of NDRG1 [5]. Although iron chelator-induced overexpression of NDRG1 is an attractive method for cancer treatment, the signaling cascade from iron depletion stress to growth-inhibitory signaling has not been defined.

Iron has an inhibitory effect on adenylyl cyclase (AC), but this effect was shown to be antagonized by stimulation of the G-protein alpha subunit (Gα), which activates AC [6]. In contrast to iron, iron chelators may activate AC and additional downstream targets such as cAMP-dependent protein kinase (PKA) and cAMP response element-binding protein (CREB) by modulating G-protein signaling. Surprisingly, it has been reported that CREB binds to cAMP response elements as well as hypoxia response elements (HREs) [7]. Since NDRG1 possesses putative HREs, it is possible that CREB directly promotes NDRG1 expression [8]. Therefore, we postulated that iron chelators induce NDRG1 overexpression through the AC-PKA-CREB signaling cascade via termination of Gαi signaling, which has an inhibitory effect on AC [9,10].

Abbreviations: AC, adenylyl cyclase; CCI, CREB-CBP binding inhibitor; CCK-8, cell counting kit-8; CREB, cAMP response element-binding protein; CSM, cysteine string motif; DDA, 2′,5′-dideoxyadenosine; DFO, desferrioxamine; FAC, ferric ammonium citrate; GAP, GTPase-activating protein; GIPN, GAIP interacting protein N terminus; Gα, G-protein alpha subunit; HIF-1α, hypoxia-inducible factor 1α; HRE, hypoxia response element; ICP-MS, inductively coupled plasma–mass spectrometry; MBP, maltose-binding protein; NDRG1, N-myc downstream-regulated gene 1 protein; PKA, cAMP-dependent protein kinase; PCR, polymerase chain reaction; RGS, regulator of G-protein signaling.

* Corresponding author.
E-mail address: slee@knu.ac.kr (S. Lee).

http://dx.doi.org/10.1016/j.bbrc.2015.06.109
0006-291X/

Regulators of G-protein signaling (RGS proteins) constitute a large family of proteins containing a ~130 amino acid RGS or RGS-like domain. Through GTPase-activating protein (GAP) activity of the conserved domain, RGS proteins facilitate the hydrolysis of GTP bound to the active Gα subunit, resulting in the termination of G-protein signaling [11]. Among a large number of RGS family members, RGS19 has the strongest interaction with Gαi3; this interaction results in termination of the inhibitory Gαi3 signal [12]. Considering these findings, we postulated that RGS19 activates the AC-PKA-CREB-NDRG1 signaling cascade by inhibiting Gαi3.

RGS19 belongs to the RZ/A subfamily, which is characterized by a highly conserved cysteine string motif (CSM) at the N-terminus. The CSM is not found in other RGS subfamilies. Moreover, this motif is completely conserved among RZ/A subfamily members in several different species [11]. Although the CSM is very short, most of the cysteine residues of RGS19 are found in this region: 8 of 11 are located in the CSM, 2 are found between the CSM and the RGS domain, and 1 is located in the RGS domain. We focused on the highly conserved and condensed CSM as a potential target site for the regulation of RGS19 function. Interestingly, the CSM of RGS19 possesses a consensus iron–sulfur binding motif (CXXCXXC), implying that RGS19 may be regulated by cellular iron availability [13].

In the present study, RGS19 was analyzed as a possible key molecule for sensing cellular iron availability. We determined that the CSM of RGS19 is an iron-incorporating domain and that RGS19 plays an important role in iron chelator-induced overexpression of NDRG1.

2. Materials and methods

2.1. Cell culture, transfection, and treatments

HeLa cells were cultured in complete minimum essential medium containing 10% fetal bovine serum, 100 units/mL penicillin, and 100 ug/mL streptomycin (Thermo Fisher Scientific, Waltham, MA, USA) at 37 °C in ambient air with 5% CO_2. Plasmid transfection was performed using FuGENE HD Transfection Reagent (Promega, Fitchburg, WI, USA) according to the manufacturers' instructions. Cells were treated with 100 μg/mL ferric ammonium citrate (FAC; Thermo Fisher Scientific); 100 μM desferrioxamine mesylate (DFO; Sigma–Aldrich, St. Louis, MO, USA); various concentrations of 2′,5′-dideoxyadenosine (DDA), H-89, or CREB-CBP binding inhibitor (CCI; Millipore, Billerica, MA, USA); and/or 25 μM MG132 (Enzo Life Sciences, Farmingdale, NY, USA).

2.2. Plasmid construction and site-directed mutagenesis

The full-length RGS19 mRNA sequence (NM_005873) flanked with 5′-EcoRI and 3′-XbaI restriction sites was amplified by polymerase chain reaction (PCR) using PrimeSTAR polymerase (TaKaRa Bio, Otsu, Shiga, Japan). Purified PCR product was cloned into the pcDNA3.1/HisC mammalian expression vector (Thermo Fisher Scientific, Waltham, MA, USA) to introduce 6 × His into the N-terminus of the protein. To prepare recombinant proteins for subsequent purification, sequences encoding full-length RGS19 and the N-terminal region containing the CSM (Met1 to Thr78) were amplified by PCR. Purified PCR products were cloned into the XmnI and NcoI sites of the pMAL-c5X bacterial expression vector (New England Biolabs, Ipswich, MA, USA) to generate maltose-binding protein (MBP) fusion proteins. Site-directed mutagenesis was performed using cysteine (TGC and TGT) to serine (AGC, AGT, and TCT) substituted synthetic oligonucleotides. The codons for serine were based on human codon usage. Primer sequences were designed and modified empirically. DpnI (New England Biolabs) was used to remove parental DNA strands. The full-length Gαi3 mRNA sequence (NM_006496) flanked with 5′-EcoRI and 3′-XbaI restriction sites was amplified by PCR. Purified PCR product was cloned into the p3 × FLAG-CMV-10 mammalian expression vector (Sigma–Aldrich, St. Louis, MO, USA) to introduce 3 × FLAG into the N-terminus of the protein. A sequence encoding full-length GAIP interacting protein N terminus (GIPN; NM_014028) flanked by 5′-EcoRI and 3′-XbaI restriction sites was amplified by PCR. Purified PCR product was cloned into a pcDNA3.1(+)/myc-HisA mammalian expression vector (Thermo Fisher Scientific) slightly modified by the insertion of a stop codon in the 3′ region of myc to remove the 6 × His tag. All constructs were verified by sequencing.

2.3. Construction of short hairpin RNA (shRNA)

Oligonucleotides 5′-GCCAGATCTGCGAGGAGAACATGCTCTTCTTTCAAGAGAAGAAGA-3′ and 5′-CGGAAGCTTAAAAAGCGAGGAGAACATGCTCTTCTTCTCTTGAAA-3′ were synthesized and annealed to produce a double-stranded shRNA template, which was amplified by PCR. Purified shRNA was digested with BglII and HindIII and inserted into pSUPER-retro-GFP/Neo. Constructs were verified by sequencing.

2.4. Total RNA isolation and quantitative real-time PCR

Total RNA was isolated from cells treated with 100 μg/mL FAC or 100 μM DFO for 6 h using an RNeasy Mini Kit (QIAGEN, Venlo, the Netherlands). After single-stranded cDNA synthesis using SuperScript II Reverse Transcriptase (Thermo Fisher Scientific, Waltham, MA, USA), a PCR mixture was prepared using SYBR Premix Ex Taq (TaKaRa Bio, Otsu, Shiga, Japan). The PCR mixture (25 μL) contained 1 × SYBR Premix Ex Taq, 0.2 μM of each primer, and template (10 ng). PCR was performed using a StepOnePlus Real-Time PCR System (Thermo Fisher Scientific). Expression levels of each gene were normalized to expression of the β-actin gene in the same preparation.

2.5. Immunoblotting

Cell lysates were prepared on ice using lysis buffer (20 mM Tris, 300 mM NaCl, 0.5% Triton X-100, and protease inhibitor cocktail; Hoffmann-La Roche, Basel, Switzerland). After removal of cell debris, quantified lysates were mixed with Laemmli sample buffer and boiled for 5 min. Proteins were separated by SDS-PAGE and transferred onto Immobilon-P PVDF membranes (Millipore, Billerica, MA, USA). For protein detection, we used primary antibodies to RGS19, GIPN, His, myc (Abcam, Cambridge, UK), p21, FLAG (Cell Signaling Technology, Danvers, MA, USA), NDRG1, and α-tubulin (Bioworld Technology, St. Louis Park, MN, USA) and appropriate secondary antibodies conjugated with horseradish peroxidase. Proteins were visualized with Clarity Western ECL Substrate (Bio-Rad Laboratories, Hercules, CA, USA). Images were acquired using a Davinch-Chemi Imager, and densitometry analysis was performed using ImageJ [14].

2.6. Assessment of viability

Cells were transfected with control vector or His-RGS19 expression vector and incubated for the indicated times in a 96-well plate. Ten microliters of cell counting kit-8 (CCK-8) solution (Dojindo Molecular Technologies, Kamimashiki, Kumamoto, Japan) was added to each well and cells were incubated for 1 h. Absorbance at 450 nm was measured using a microplate reader.

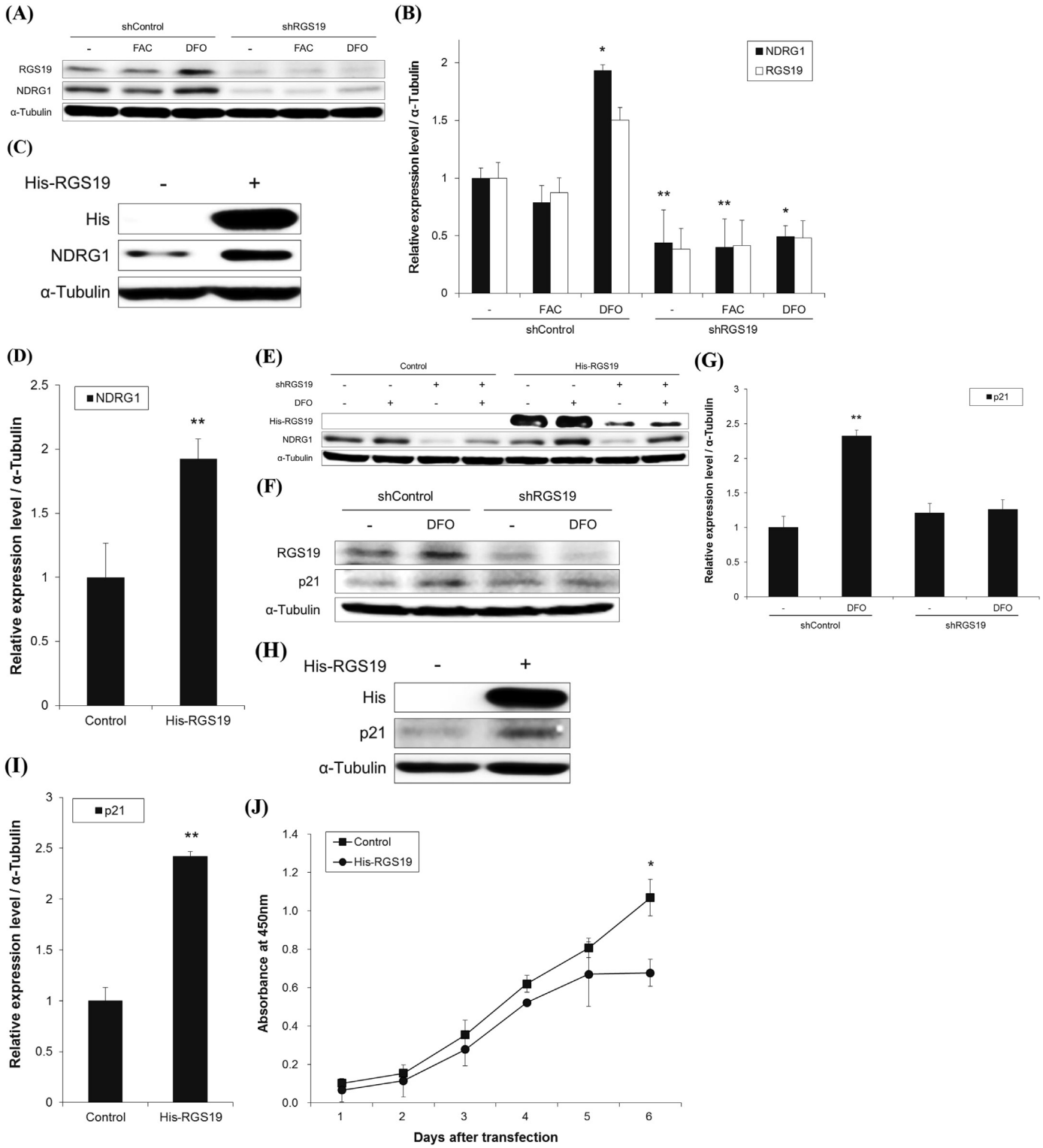

Fig. 1. RGS19 is required for DFO-induced overexpression of NDRG1 and p21. (A, F) After HeLa cells stably expressing control or RGS19 shRNA were treated with 100 μg/mL FAC or 100 μM DFO for 6 h, endogenous protein levels of RGS19, NDRG1, and p21 were analyzed. (C, H) Control vector or His-RGS19 expression vector was transfected into HeLa cells and expression levels of His-RGS19, NDRG1, and p21 were analyzed. (E) HeLa cells stably expressing RGS19 shRNA were transfected with control vector or His-RGS19 expression vector and treated with DFO. The expression level of NDRG1 was analyzed. (B, D, G, I) Densitometry analysis of the protein levels of RGS19, NDRG1, and p21. (J) HeLa cells were transfected with control vector or His-RGS19 expression vector for the indicated times and viability was analyzed using a CCK-8 kit.

2.7. Purification of recombinant proteins

Recombinant protein expression and purification were performed according to the manufacturer's instructions. Briefly, *Escherichia coli* 2523 cells (New England Biolabs, Ipswich, MA, USA) transformed with wild-type or mutant constructs were inoculated into LB broth (10 g tryptone, 5 g yeast extract, 5 g sodium chloride, 2 g glucose, and 100 mg ampicillin per liter) and incubated overnight at 37 °C with shaking. Overnight cultures were inoculated into fresh medium and incubated for another 1.5 h. Protein expression was induced by adding 0.3 mM IPTG and incubating for an additional 3 h. Cells were harvested, resuspended in lysis buffer (20 mM Tris, pH 8.0, 1 M NaCl), and sonicated until protein release reached a maximum level. Soluble fractions were loaded on amylose resin and columns were washed intensively. MBP-tagged proteins were recovered with elution buffer (20 mM Tris, pH 8.0, 1 M NaCl, 10 mM maltose; Sigma–Aldrich, St. Louis, MO, USA).

2.8. Inductively coupled plasma–mass spectrometry (ICP-MS)

To minimize signal variation caused by any solute in the buffer, purified MBP-tagged proteins (200 μg/mL) were intensively dialyzed against double-distilled water using an Amicon Ultra 0.5 mL 3 K centrifugal filter (Millipore, Billerica, MA, USA). Proteins were mixed with 8 volumes of 2% OPTIMA-grade nitric acid. Subsequently, 20 μL of a 5-ppm aqueous scandium ion solution (ICP-MS grade) was added to each tube as an internal standard and contents were mixed vigorously. ICP measurements were then conducted on a NexION 300X ICP-MS spectrometer (PerkinElmer, Waltham, MA, USA) in extended dynamic range mode. Reported measurements of iron in each sample represent the mean of 3 measurements. Individual measurements were typically obtained with a relative standard deviation of approximately 3% or less per sample. An equivalent amount of purified protein (2.5 μg/lane) was separated by SDS-PAGE and stained with Coomassie Brilliant Blue (Sigma–Aldrich, St. Louis, MO, USA) to verify quality and quantity.

2.9. UV–visible absorption spectra

Purified RGS19 and C135S or CSM deletion mutants (10 mg/mL) were dialyzed against 20 mM Tris, pH 7.5, 150 mM NaCl buffer and treated with or without 5 mM sodium dithionite (Sigma–Aldrich, St. Louis, MO, USA) for 1 h. Absorption spectra from 280 nm to 700 nm were obtained with a NanoVue spectrometer (GE Healthcare, Little Chalfont, UK).

2.10. GTPase-activating protein activity

GAP activity of MBP-tagged RGS19, C135S, and CSM deletion mutants was analyzed using a High Throughput Colorimetric GTPase Assays kit (Innova Biosciences, Cambridge, UK). Purified Gαi3-His (1 μM) was prepared as a substrate in 50 mM Tris, pH 7.5, 2.5 mM $MgCl_2$, 0.5 mM GTP, and 0.5 mM β-mercaptoethanol. Gαi3-His was pre-charged with GTP at 4 °C for 1 h and then 2 μM wild-type or mutant RS19 was added. After incubation for 1 h at room temperature, PiColorLock Gold reagent and stabilizer were added. The absorbance at 590 nm of a non-substrate control was subtracted.

2.11. Data analysis

Data are presented as the mean ± standard deviation of at least three independent experiments. Statistical significance was

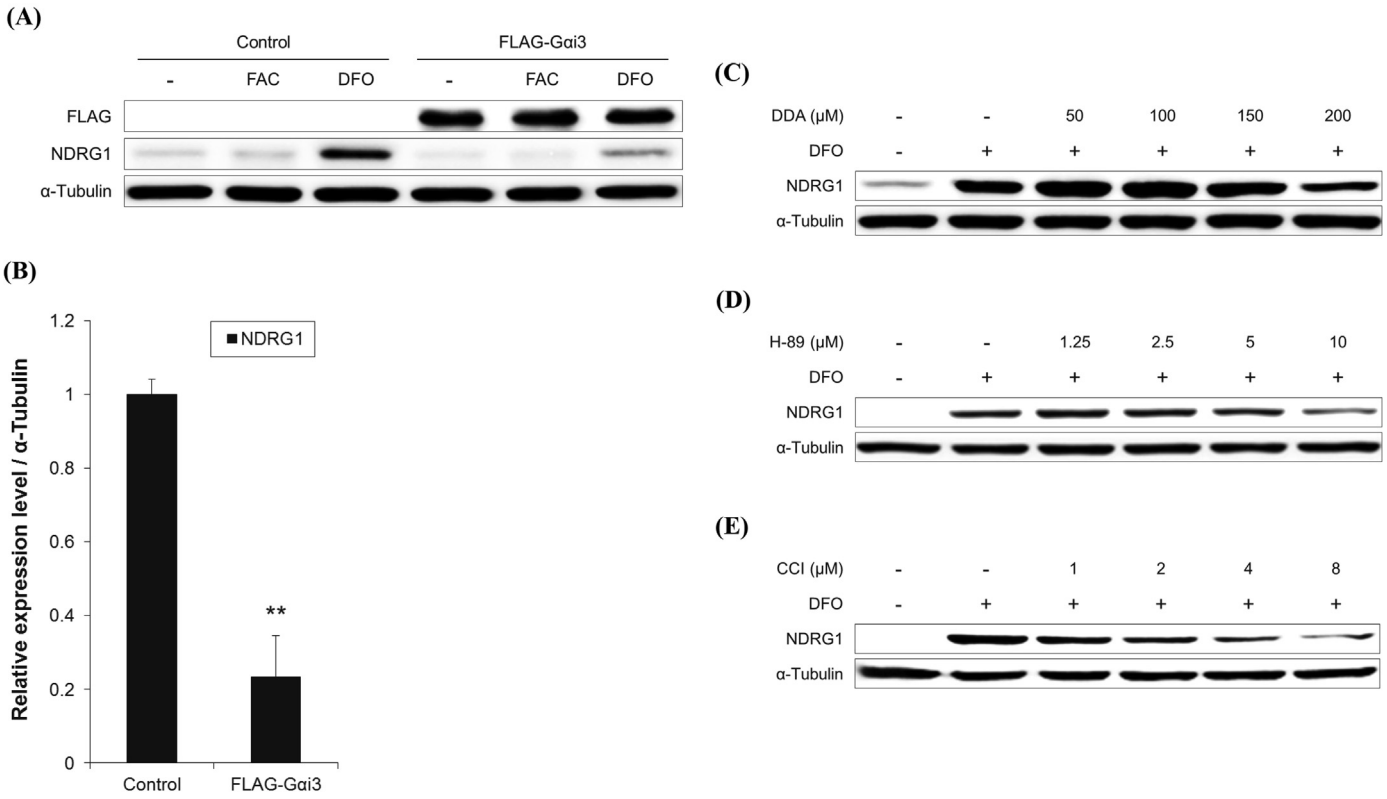

Fig. 2. DFO induces overexpression of NDRG1 through the G-protein signaling cascade. (A) HeLa cells expressing 3 × FLAG-tagged Gαi3 were treated with 100 μg/mL FAC or 100 μM DFO for 6 h and the endogenous expression pattern of NDRG1 was analyzed. (B) Densitometry analysis of DFO-induced expression of NDRG1 in HeLa cells overexpressing FLAG-Gαi3. HeLa cells were pretreated with DMSO or various concentrations of DDA (C), H-89 (D), or CCI (E) for 1 h, followed by treatment with 100 μM DFO.

analyzed using Student's *t* test. ** indicates $P < 0.01$ and * indicates $P < 0.05$. All experiments were performed at least in triplicate.

3. Results

3.1. DFO induces NDRG1 expression through RGS19, resulting in inhibition of cell proliferation

To determine whether RGS19 participates in DFO-induced NDRG1 overexpression, control vector or shRNA against RGS19 was transfected into HeLa cells and selection was performed to establish a cell line stably expressing RGS19 shRNA. DFO-induced iron deprivation stress significantly increased the NDRG1 expression level in control cells (1.9-fold). However, when endogenous RGS19 was downregulated, DFO-induced overexpression of NDRG1 was significantly reduced (Fig. 1A and B). Conversely, when RGS19 was overexpressed, NDRG1 expression was significantly upregulated without DFO (Fig. 1C and D). These results indicate that RGS19 plays an important role in the signaling cascade of iron chelation-induced NDRG1 overexpression. Ectopic expression of His-RGS19 partially restored the NDRG1 expression level (Fig. 1E and Supplementary Fig. 1).

Previously, NDRG1 was reported to be an inducer of p21, one of the cyclin-dependent kinase inhibitors [4]. In DFO-treated cells, NDRG1 was overexpressed and p21 was significantly upregulated. However, the increased expression of p21 was abolished by the knockdown of RGS19 (Fig. 1F and G). These results indicate that RGS19 is required for DFO-induced overexpression of NDRG1 target genes. As expected, ectopic expression of His-RGS19 increased the protein level of p21 (Fig. 1H and I). The viability of cells expressing His-RGS19 was significantly decreased (around 1.5-fold) 6 days after transfection (Fig. 1J). The growth-inhibitory effect of His-RGS19 was also confirmed in the SW480 cell line (Supplementary Fig. 2). These results indicate that RGS19 promotes a growth-inhibitory signal, possibly through an NDRG1 target, the p21 gene.

3.2. Iron depletion stress induces NDRG1 overexpression via the G-protein signaling cascade

We postulated that G-protein signaling may be related to the DFO-RGS19-NDRG1 signaling cascade as a target of RGS19. To confirm this hypothesis, HeLa cells expressing Gαi3 were treated with DFO to induce NDRG1 expression. DFO-induced overexpression of NDRG1 was significantly reduced by Gαi3 (Fig. 2A

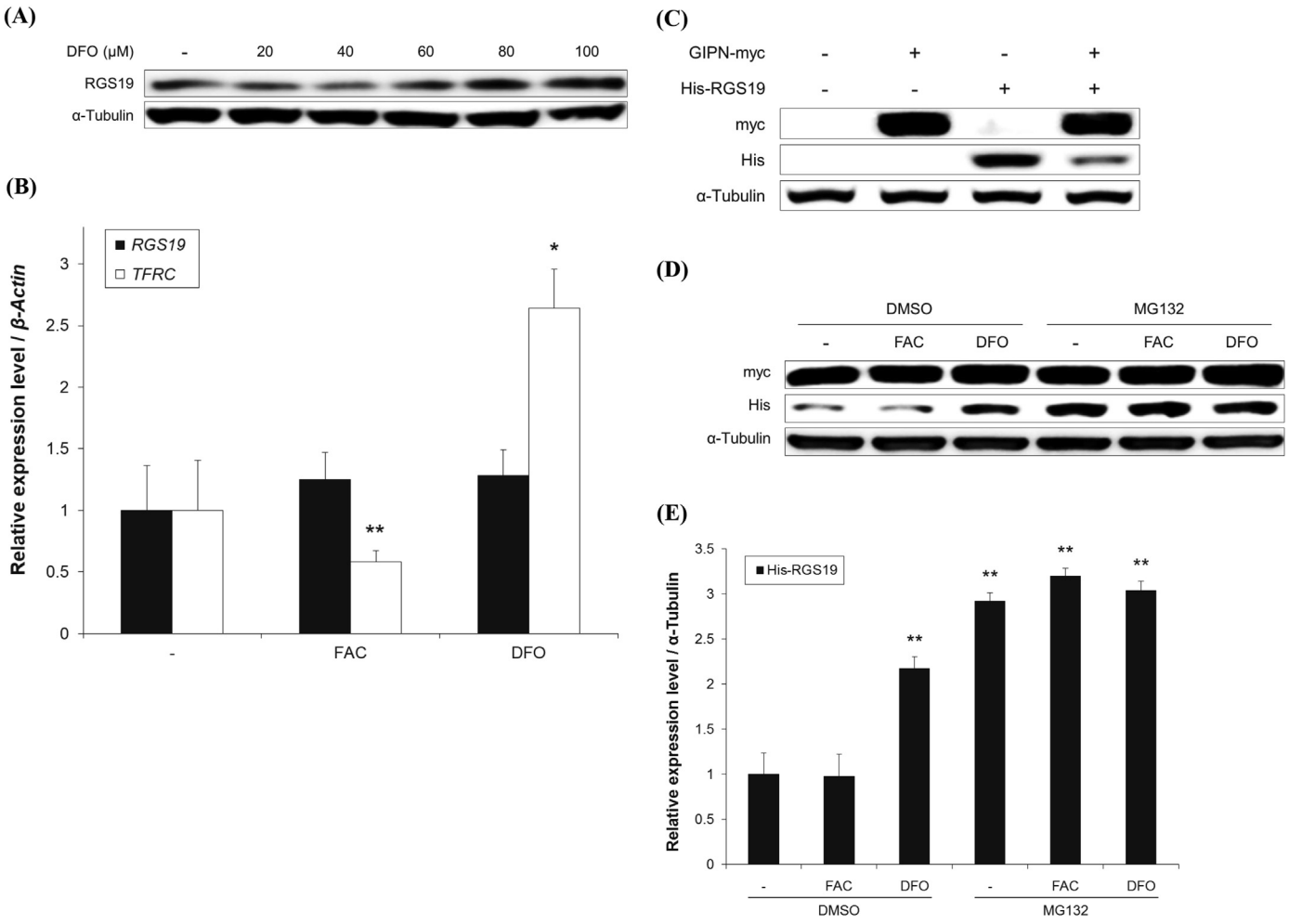

Fig. 3. The stability of RGS19 is regulated by GIPN through cellular iron availability. (A) HeLa cells were treated with various concentrations of DFO for 6 h and the endogenous protein level of RGS19 was analyzed. (B) After treatment with 100 μg/mL FAC or 100 μM DFO for 6 h, total RNA was isolated and cDNA was synthesized. The expression levels of endogenous *RGS19*, transferrin receptor (*TFRC*), and *β-actin* genes were analyzed. The *TFRC* gene was used as a DFO-induced positive control. (C) His-RGS19 was co-expressed with or without GIPN-myc for 24 h and expression levels of His-RGS19 and GIPN-myc were detected using antibodies against His and myc, respectively. (D) Cells were co-transfected with His-RGS19 and GIPN-myc expression vectors and treated with 100 μg/mL FAC or 100 μM DFO for 6 h with or without MG132. (E) Densitometry analysis of the protein level of His-RGS19 in cells co-transfected with GIPN-myc and treated with FAC or DFO with or without MG132.

and B). This implies that RGS19 propagates DFO-induced growth-inhibitory signaling by inactivating the negative regulator Gαi3. Additionally, the involvement of downstream targets of Gαi3 was analyzed. AC, PKA, and CREB activities were specifically inhibited by DDA, H-89, and CCI, respectively. We found that DFO-induced overexpression of NDRG1 was significantly reduced by DDA, H-89, and CCI in a dose-dependent manner (Fig. 2C–E). These results indicate that the RGS19-Gαi3-AC-PKA-CREB signaling cascade

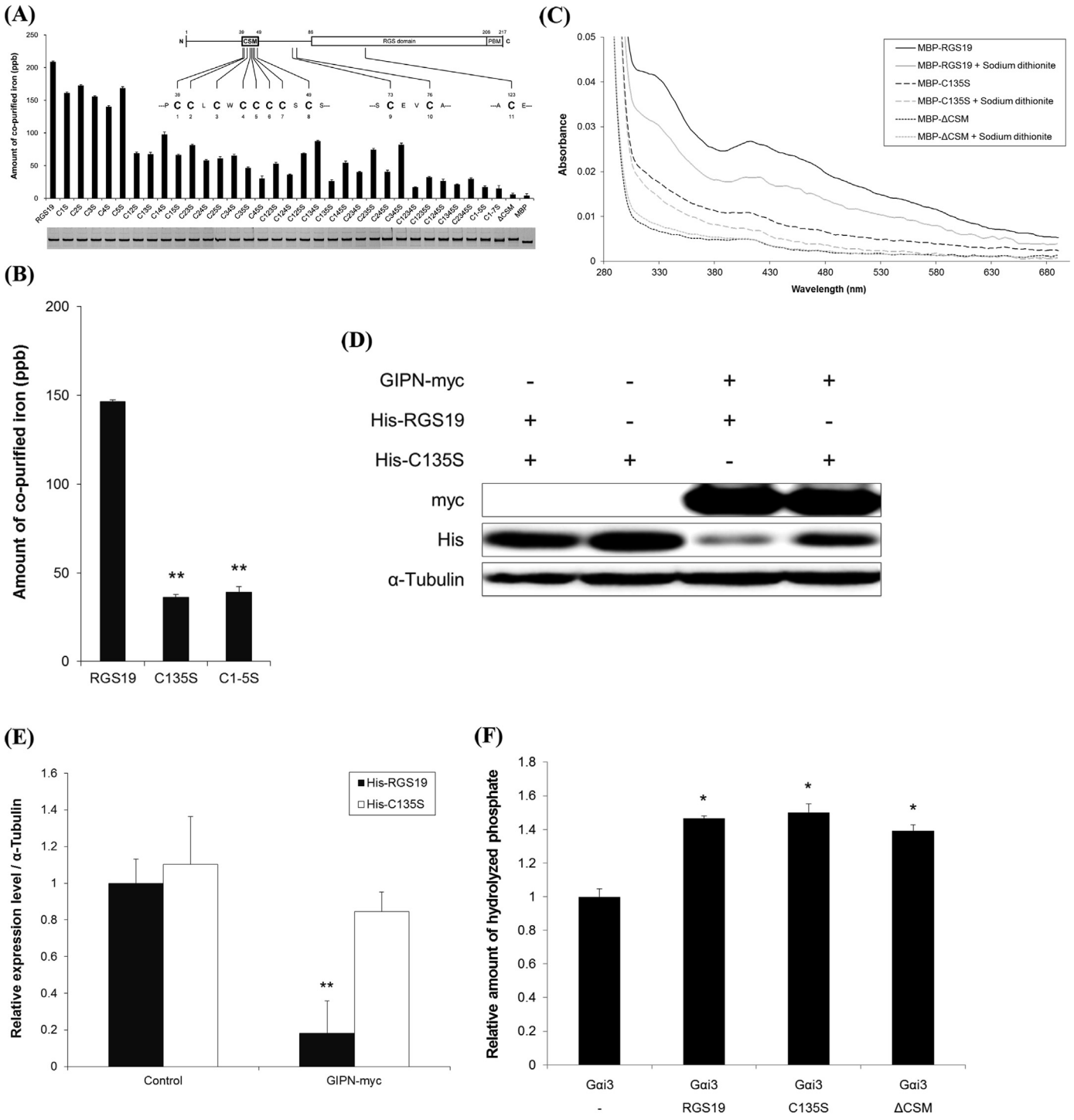

Fig. 4. Iron is incorporated into the CSM of RGS19. (A) CSM of wild-type RGS19 and mutants were purified (200 μg/mL) and subjected to ICP-MS. The basal level of iron contained in the reaction buffer was subtracted and MBP was used as a negative control. The number and distribution of cysteine residues are shown at the top. The first N-terminal cysteine residue (C39) is numbered as 1. The quality and quantity of purified proteins were verified by Coomassie Brilliant Blue staining (bottom). (B) Full-length wild-type RGS19 and mutants were purified and subjected to ICP-MS. The basal level of iron contained in the reaction buffer was subtracted and MBP was used as a negative control. (C) Purified (10 mg/mL) full-length RGS19 (solid line) and C135S (dashed line) and ΔCys (dotted line) mutants were treated with (grey line) or without (black line) 5 mM sodium dithionite. UV–visible absorption spectra of the purified proteins revealed major peaks around 325 and 420 nm and shoulders around 460 and 550 nm. (D and E) Expression levels of His-RGS19 and His-C135S with or without co-expressed GIPN-myc. (F) GAP activity of MBP-RGS19 was analyzed by measuring the amount of hydrolyzed phosphate from pre-charged Gαi3-His.

plays a role in the induction of iron depletion-induced stress signaling.

3.3. GIPN regulates the stability of RGS19 through cellular iron availability

Interestingly, the endogenous protein level of RGS19 was increased by DFO treatment (Fig. 1A). To analyze the mechanism by which DFO induces upregulation of endogenous RGS19, cells were treated with DFO at different doses. The level of endogenous RGS19 was significantly increased by DFO in a dose-dependent manner (Fig. 3A). However, transcription of *RGS19* was not altered, whereas transcription of the transferrin receptor gene (*TFRC*), which encodes the carrier responsible for iron uptake, was significantly increased under iron-depleted conditions (Fig. 3B). These results indicate that iron depletion may enhance protein stability but has no effect on the transcription of *RGS19*.

Co-expression of GIPN-myc significantly decreased the expression level of His-RGS19 (Fig. 3C). However, DFO antagonized the negative effect of GIPN-myc on His-RGS19 stability. The specific proteasome inhibitor MG132 protected RGS19 from GIPN-induced downregulation (Fig. 3D and E). These results indicate that RGS19 may be targeted for proteasomal degradation by GIPN but is stabilized under iron-depleted conditions.

3.4. RGS19 incorporates iron through the CSM and shows characteristics of iron-binding proteins

Since iron chelation has a protective effect on RGS19, we postulated that iron is incorporated into RGS19 as a key molecule that determines protein stability. To test this hypothesis, we purified recombinant CSM and measured the amount of co-purified iron. Site-directed mutagenesis was performed to generate combinatorial mutant constructs. Recombinant wild-type CSM and cysteine-to-serine substituted mutants CSMs were produced and subjected to ICP-MS (Fig. 4A). The results indicated that a single cysteine mutation had no significant effect on iron incorporation, as mutants with a single substitution were co-purified with a significant amount of iron. However, as the number of mutated residues increased, the amount of co-purified iron was significantly reduced. A single mutation reduced the amount of co-purified iron by approximately 25%, and double and triple mutations reduced the amount by approximately 50–70%. When more than 4 cysteine residues were substituted, the iron content was dramatically reduced. The arrangement of 1st, 3rd, and 5th cysteine residues (C135) in CSM (CXXCXXC, Fig. 4A inlet) is similar to those of iron–sulfur binding proteins. Similar to CSM, the amount of iron was significantly reduced in the full-length C135S mutant (Fig. 4B). UV–visible absorption spectra indicated that RGS19 has peaks around 325, 420, 460, and 550 nm (Fig. 4C; black solid line), which is characteristic of [2Fe–2S] cluster-containing proteins [15]. However, the C135S and CSM deletion (ΔCys) mutants did not have such a pattern (Fig. 4C; black dashed and dotted lines). Furthermore, sodium dithionite-mediated reduction diminished these characteristics (Fig. 4C; grey lines). These results suggest that the 1st, 3rd, and 5th cysteines are pivotal residues for incorporation of iron into RGS19.

To confirm that iron is required for the degradation of RGS19, wild-type RGS19 or the C135S mutant was co-expressed with GIPN. The expression of His-C135S was moderately downregulated by GIPN-myc, whereas His-RGS19 expression was significantly downregulated, by more than 80% (Fig. 4D and E). Interestingly, GAP activity of MBP-RGS19 was not altered by cysteine substitution or CSM deletion (Fig. 4F). These results confirm that iron incorporation is required for GIPN-dependent degradation of RGS19.

4. Discussion

HeLa cells were used in this study because this cell line expresses endogenous RGS19 and GIPN. When His-RGS19 or His-C135S was co-expressed with GIPN-myc, the protein level was significantly reduced for His-RGS19 but retained for His-C135S. To mimic co-expression with GIPN-myc, His-RGS19 and His-C135S expression vectors were transfected into other cell lines that express endogenous GIPN more strongly than HeLa cells do. In SW480 and HEK293 cells, His-RGS19 had a significantly lower expression level than His-C135S without ectopic expression of GIPN (Supplementary Fig. 3).

Interestingly, intensive mutagenesis revealed that C1–5S and C1–7S, including other moderate iron-free mutants, were still co-purified with a trace of iron whereas the CSM-deleted mutant contains negligible amount of iron (Fig. 4A). This result indicates that remaining cysteine residues may act as supporting sulfur donor for iron incorporation.

HREs have been found in the promoter region of *NDRG1* at −1376 bp and −7503 bp. Additionally, hypoxia-inducible factor 1α (HIF-1α) was previously determined to be a transcription factor for *NDRG1* [16,17]. Although *NDRG1* does not possess a cAMP response element, it was reported that CREB also binds to the HIF-1α response element and significantly enhanced the expression of HRE-controlled luciferase in HeLa cells treated with a cAMP analog [7]. Moreover, a previous report described the induction of NDRG1 expression by an iron chelator in HIF-1α$^{-/-}$ murine embryo fibroblasts [8]. These reports suggest that an iron chelator may induce NDRG1 expression through CREB in addition to HIF-1α. Although partial induction of NDRG1, putatively by HIF-1α, was detected in cells transfected with RGS19 shRNA (Fig. 1A), ectopic expression of His-RGS19 significantly enhanced the expression level of NDRG1 and its downstream target genes without iron chelation. Together, these results suggest that NDRG1 could be regulated by CREB and that this regulatory mechanism is controlled by iron-sensitive RGS19.

Although iron chelation is a promising cancer treatment, chelating drugs can cause side effects such as visual disturbances, vomiting, diarrhea, stomach or leg cramps, rapid heartbeat, hypotension, anaphylactic shock, and pain or swelling at the site of intravenous entry. Therefore, it is important to understand iron chelator-induced antiproliferative mechanisms and find new molecular targets. In this study, we found that RGS19 is involved in iron deprivation-induced growth-inhibitory signaling, which suggests that specific chemicals that increase the expression level of endogenous RGS19 may be useful for cancer treatment.

Acknowledgments

This study was supported by a grant from the Technology Innovation Program (10038744) of the Korea Evaluation Institute of Industrial Technology, funded by the Ministry of Trade, Industry & Energy, Republic of Korea.

Appendix A. Supplementary data

Supplementary data related to this article can be found at http://dx.doi.org/0.10.1016/j.bbrc.2015.06.109.

Transparency document

Transparency document related to this article can be found online at http://dx.doi.org/0.10.1016/j.bbrc.2015.06.109.

References

[1] Z. Kovacevic, D.S. Kalinowski, D.B. Lovejoy, Y. Yu, Y. Suryo Rahmanto, P.C. Sharpe, P.V. Bernhardt, D.R. Richardson, The medicinal chemistry of novel iron chelators for the treatment of cancer, Curr. Top. Med. Chem. 11 (2011) 483–499.

[2] J.L. Kim, H.N. Kang, M.H. Kang, Y.A. Yoo, J.S. Kim, C.W. Choi, The oral iron chelator deferasirox induces apoptosis in myeloid leukemia cells by targeting caspase, Acta Haematol. 126 (2011) 241–245.

[3] M.P. Tschan, D. Shan, J. Laedrach, M. Eyholzer, E.O. Leibundgut, G.M. Baerlocher, A. Tobler, D. Stroka, M.F. Fey, NDRG1/2 expression is inhibited in primary acute myeloid leukemia, Leukemia Res. 34 (2010) 393–398.

[4] Z. Kovacevic, S. Sivagurunathan, H. Mangs, S. Chikhani, D. Zhang, D.R. Richardson, The metastasis suppressor, N-myc downstream regulated gene 1 (NDRG1), upregulates p21 via p53-independent mechanisms, Carcinogenesis 32 (2011) 732–740.

[5] B.A. Fang, Z. Kovacevic, K.C. Park, D.S. Kalinowski, P.J. Jansson, D.J. Lane, S. Sahni, D.R. Richardson, Molecular functions of the iron-regulated metastasis suppressor, NDRG1, and its potential as a molecular target for cancer therapy, Biochimica biophysica acta 1845 (2014) 1–19.

[6] A. Moser, O. Schuster, Iron inhibits D-1 dopamine receptor coupled adenylate cyclase via G-proteins in the caudate nucleus of the rat, Biochem. Biophys. Res. Commun. 171 (1990) 1372–1377.

[7] I. Kvietikova, R.H. Wenger, H.H. Marti, M. Gassmann, The transcription factors ATF-1 and CREB-1 bind constitutively to the hypoxia-inducible factor-1 (HIF-1) DNA recognition site, Nucleic Acids Res. 23 (1995) 4542–4550.

[8] N.T. Le, D.R. Richardson, Iron chelators with high antiproliferative activity up-regulate the expression of a growth inhibitory and metastasis suppressor gene: a link between iron metabolism and proliferation, Blood 104 (2004) 2967–2975.

[9] R. Taussig, J.A. Iniguez-Lluhi, A.G. Gilman, Inhibition of adenylyl cyclase by Gi alpha, Science 261 (1993) 218–221.

[10] C.W. Dessauer, M. Chen-Goodspeed, J. Chen, Mechanism of galpha i-mediated inhibition of type V adenylyl cyclase, J. Biological Chem. 277 (2002) 28823–28829.

[11] N. Watson, M.E. Linder, K.M. Druey, J.H. Kehrl, K.J. Blumer, RGS family members: GTPase-activating proteins for heterotrimeric G-protein alpha-subunits, Nature 383 (1996) 172–175.

[12] L. De Vries, M. Mousli, A. Wurmser, M.G. Farquhar, GAIP, a protein that specifically interacts with the trimeric G protein G alpha i3, is a member of a protein family with a highly conserved core domain, Proc. Natl. Acad. Sci. U. S. A. 92 (1995) 11916–11920.

[13] M.L. Antonkine, M.S. Koay, B. Epel, C. Breitenstein, O. Gopta, W. Gartner, E. Bill, W. Lubitz, Synthesis and characterization of de novo designed peptides modelling the binding sites of [4Fe-4S] clusters in photosystem I, Biochimica Biophysica acta 1787 (2009) 995–1008.

[14] C.A. Schneider, W.S. Rasband, K.W. Eliceiri, NIH image to ImageJ: 25 years of image analysis, Nat. Methods 9 (2012) 671–675.

[15] N.P. Tucker, M.G. Hicks, T.A. Clarke, J.C. Crack, G. Chandra, N.E. Le Brun, R. Dixon, M.I. Hutchings, The transcriptional repressor protein NsrR senses nitric oxide directly via a [2Fe-2S] cluster, PLoS One 3 (2008) e3623.

[16] D. Wei, J.J. Peng, H. Gao, H. Li, D. Li, Y. Tan, T. Zhang, Digoxin downregulates NDRG1 and VEGF through the inhibition of HIF-1alpha under hypoxic conditions in human lung adenocarcinoma A549 cells, Int. J. Mol. Sci. 14 (2013) 7273–7285.

[17] Q. Wang, L.H. Li, G.D. Gao, G. Wang, L. Qu, J.G. Li, C.M. Wang, HIF-1alpha up-regulates NDRG1 expression through binding to NDRG1 promoter, leading to proliferation of lung cancer A549 cells, Mol. Biol. Reports 40 (2013) 3723–3729.